



Parametric characterization of a mesomechanic kinematic caused by ondulation in fabric reinforced composites: analytical and numerical investigations

Marco Romano, Ingo Ehrlich

Ostbayerische Technische Hochschule Regensburg, Department of Mechanical Engineering, Laboratory of Composite Technology, Galgenbergstrasse 30, 93053 Regensburg, Germany

Norbert Gebbeken

University of the Bundeswehr Munich, Department of Civil Engineering and Environmental Sciences, Institute of Engineering Mechanics and Structural Analysis, Werner-Heisenberg-Weg 39, 85577 Neubiberg, Germany

ABSTRACT. A parametric characterization of a mesomechanic kinematic caused by ondulation in fabric reinforced composites is investigated by analytical and numerical investigations. Due to the definition of plain representative sequences of balanced plain-weave fabric reinforced single layers based on sines the variable geometric parameters are the amplitude and the length of the ondulation. The mesomechanic kinematic can be observed in both the analytic model and the FE-analyses. The analytic model yields hyperbolic correlations due to the strongly simplifying presumptions that neglect elasticity. In contrast the FE-analyses yield linear correlations in much smaller amounts due to the consideration of elastic parts, yet distinctly.

KEYWORDS. Fiber reinforced plastics; Mesomechanic scale; Fabric reinforced layer; Ondulation.



Citation: Romano, M., Ehrlich, I., Gebbeken, N., Parametric characterization of a mesomechanic kinematic caused by ondulation in fabric reinforced composites: analytical and numerical investigations, *Frattura ed Integrità Strutturale*, 39 (2017) 226-247.

Received: 29.09.2016

Accepted: 02.12.2016

Published: 01.01.2017

Copyright: © 2017 This is an open access article under the terms of the CC-BY 4.0, which permits unrestricted use, distribution, and reproduction in any medium, provided the original author and source are credited.

INTRODUCTION

Nowadays the use of fiber reinforced plastics become indispensable in many areas in industry. The feature of high stiffness and strength which simultaneously combine low mass allows new design approaches for weight loss, which leads to energy savings, for example in the automotive and aircraft industry.

Simplified theoretical approaches for fiber reinforced plastics often presume a layout of only unidirectionally reinforced single layers. As a first approach in applied engineering the structural mechanic properties can analytically be determined by the use of so-called micromechanical homogenization theories. These are usually based on the single components' properties, namely matrix and fiber. However, different kinds of fabrics are often applied as reinforcements in the layout of structural parts. In this case homogenization theories reach their limit. The reason therefore is that the mesomechanic



geometry of fabric reinforced single layers cannot be considered sufficiently by relatively simple homogenization approaches. Yet, mesomechanic correlations are distinctly different as they significantly influence the mechanical properties of a structure.

RESEARCH ENVIRONMENT

The research environment is the description of the structural mechanic behavior of fabric reinforced plastics. A chronological literature review is presented. The conclusions lead to the pursued mechanical principle.

Literature review

Naik and Shembekar 1992 [1] present linear-elastic investigations of plain-weave fabric reinforced single layers. The ondulation influences the plane structural mechanical material properties. There is a significant discrepancy between the one-dimensional analytical and numerical investigations to them of the experiments. In contrast the two-dimensional analytical and numerical investigations correlate very well with the experiments.

Mital, Murthy and Chamis 1996 [2] investigate the micromechanics of plain weave composites. As a result the effects of the fabric reinforcement have been described analytically and basically verified numerically. The fiber-orientation in the mesoscopic dimension has been described by sinusoid parts in the ondulation region connected by straight parts above and under the ondulated yarn. For means of simplicity and in order to reduce computation time symmetry characteristics has been used in the model.

Guan 1997 [3] investigates the visco-elastic damping in fabric reinforced single layers by FE-calculations. A plain-weave fabric is modeled by representative volume elements. A sensitivity analysis regarding the length of the ondulation shows, that the model is relatively insensitive to a variation of this geometric parameter. A basic validation is carried out by the decay of vibrating flat beam-like specimens.

Byun 2000 [4] presents an analytical model of a so called unit cell in a mesomechanic scale in order to calculate the geometric characteristic and the three-dimensional structural material properties. In detail the ondulation is presumed continuously differentiable and investigated by coordinate transformation. A validation in one-dimensional tensile tests is carried out for seven different fabric constructions.

Huang 2000 [5] treats the structural mechanical properties of laminates of fabrics according to the introduced the so-called bridging model. It describes linear-elastic, plastic and strength aspects of balanced plain-weave fabrics under arbitrary loading. The presumed geometry causes three mechanically different regions, namely warp and fill yarn and surrounding matrix. Several geometric parameters are considered for a verification of the model. An experimental validation yields a good correlation with the results of the analytic model.

Guan and Gibson 2001 [6] suppose the acting of a mesomechanic mechanism for damping in fabric reinforced composites. Therefore a plain-weave construction is investigated numerically and validated basically by the decay of vibrating flat beam-like specimens.

Tabiei and Yi 2002 [7] confront different methods for the determination of structural mechanic material properties of fabric reinforced plastics, amongst representative volume elements, four-cell-method and three-dimensional FE-calculations. In detail results of different numerical investigations with FE-calculations are confronted. Besides precision the numerical efficiency and thereby the applicability is taken into account.

Le Page et al. 2004 [8] carry out two-dimensional FE-calculations, presuming plane stress and considering mesomechanic geometric parameters. The aim is the prediction of damage propagation in fabric reinforced laminates as a function of the number of layers. Thereby layups with different numbers of single layers of plane-weave fabrics are investigated under the presumption of the “in-phase” arrangement and “out-of-phase” arrangement. Against this background parametrical FE-calculations are carried out.

Wielage et al. 2005 [9] emphasize the relevance of a detailed mesomechanic description of laminates of fabric reinforced single layers. The carried out FE-calculations consider representative volume elements of three kinds of fabrics, namely plain-weave, twill 2/2 and satin 1/4. The independent structural mechanic material properties of the ondulated rovings are presumed as 0°-unidirectionally reinforced regions. The structural mechanic stiffnesses and the thermal expansion coefficients are calculated and validated experimentally.

Barbero et al. 2006 [10] describe a FE-model for the calculation of laminates of plain-weave fabrics. The basically different arrangements, namely “in-phase” (here called “iso-phase”) and “out-of-phase”, are considered. The difference between the global and local fiber volume content is discussed. The determination of the local fiber volume content in the



ondulated rovings is done by the weighted average of the experimentally determined global fiber volume content, based on the relative part of the areas of the different regions.

Ballhause 2007 [11] investigates the structural mechanics of dry fabrics on the mesomechanic scale under one- and two-dimensional loading. A failure model is formulated based on the increase of contact forces and simultaneously the reduction of the curvatures at the crossings under increasing loads.

Matsuda et al. 2007 [12] besides the elastic behavior investigate the viscoplastic parts in plain weave fabrics. A homogenization theory is developed numerically considering the in-phase and out-of-phase arrangement.

Nakanishi et al. 2007 [13] investigate the damping properties of fabric reinforced composites. Thereby glass fibers as a plain weave fabric in a polymeric matrix system are considered in numerical investigations. Based on the determined mesomechanic properties flat beam-like specimens have been modeled by means of FE-analyses and investigated up to the third bending mode in vibration.

Badel, Vidal-Sallé and Boisse 2007 [14] as well as Hivet and Boisse 2008 [15] identify a mesoscopic mechanical behavior for woven composites. Therefore dry fabrics under biaxial tension are investigated numerically. A strong nonlinearity is reported especially at the beginning of the loading.

El Mahi et al. 2008 [16] present an analytical description of structural mechanic material damping mechanisms in fabrics. The carried out FE-calculations are validated. The strain energy under the presumption of plane stress is considered. The validation is carried out by the decay of vibrating flat beam-like specimens at the first three natural frequencies. The 0°-unidirectionally reinforced specimens show smaller structural material damping as the fabric reinforced ones, whereat the plain-weave reinforced specimens showed distinctly higher damping values than the twill-fabric reinforced ones. The effect, however, is lead back to friction, what is rather improbable when the specimens originally are neither prestressed nor damaged.

Szablewski 2009 [17] treats representative sequences of plain-weave reinforced single layers under the simplifying presumption of sine-shaped undulations of the rovings in the mesomechanic scale. The geometrically definitely defined model provides the determination of stress and strength aspects. Finally, the possible adaption of the presented idealized geometry to other types of fabric constructions is mentioned.

Hivet and Duong 2010 [18] carry out similar numerical investigations for dry fabric reinforcements under shear load conditions. Thereby the load is applied by a picture-frame mechanism. Nonlinearities are detected regarding the angle of deformation and the resulting orientation of the yarns in the fabric.

Ansar, Xinwei and Chouwei 2011 [19] give a review about modeling strategies. Even if 3D woven composites are focused, a parametric consideration of the geometric dimensions is supposed. Correlations between geometric and technical parameters are indicated. Different approximations for modeling the cross-section, amongst others a lens-shaped cross-section, of the single tows are listed.

Kreikmeier et al. 2011 [20] introduce sine-shaped fiber-orientation in the in-plane direction as an imperfection due to a selected manufacturing process. The sine as an analytical function is processed analytically for a basic description of the phenomenon, yet without parametric variation of the geometric dimensions.

Valentino et al. 2013 [21] and Valentino et al. 2014 [22] mechanically characterize basalt fiber reinforced plastics with different fabric reinforcements by experimental tensile tests and FE-calculations. In ranges of small deformations and at a comparable fiber volume content the fabric reinforced specimens exhibit slightly lower stiffnesses as the comparable 0°-unidirectionally reinforced ones.

Pursued mechanical principle

The aim of the carried out investigations is the identification and verification of a mesomechanic kinematic caused by undulations in fabric reinforced composites. Based on a sine as a purely analytic trigonometric function according to Eq. (2) a so called plain representative sequence of a balanced plain weave fabric reinforced layer can be derived. The amplitude A and the length L are the characteristic geometric parameters. They define an entire cross-section of one complete undulation. Two reasonable basic geometries for further analytical processing and for the carried out FE-analyses are shown in Fig. 1 left.

The simplified geometry of the undulation for the carried out FE-analyses represents an idealized cross-section of the warp yarn of a fabric reinforced single layer cut along its theoretic center line perpendicular to the crossing fill yarns. Three structural mechanically different regions can be identified. Regarding their stiffnesses as the characteristic structural mechanical properties there are

- the warp yarn with predominant direction following the longitudinal sine and so E_1 following the sine and E_2 perpendicular to it,



- the two fill yarns with predominant direction perpendicular to the cross-section and so $E_2 = E_3$ in the investigated plain model and
- the matrix region that is not reinforced at all with E_m .

There are significant differences in the values of the stiffnesses of the different regions. Thereby the stiffness E_1 of the unidirectionally reinforced yarns is significantly higher in the direction of the reinforcement compared to the stiffness E_2 in direction perpendicular to the reinforcement and the stiffness E_m of the matrix region. The relations can mathematically be related by

$$E_1 \gg E_2 > E_m \quad (1)$$

Common homogenization theories yield $E_1 = 150 \text{ GPa} \gg E_2 = 11.5 \text{ GPa} > E_m = 3.3 \text{ GPa}$ in case of a unidirectionally reinforced single layer with high tenacity (HT) carbon fibers with a presumed fiber volume content of $\phi_f = 60\%$ as absolute values for the stiffnesses.

Two different effects in the model can be identified, when positive and negative longitudinal deformations are considered. In both cases the unidirectionally reinforced undulated yarn is subjected to a purely elastic deformation. Additionally at the same time in case of positive longitudinal deformations a smoothing or flattening, and in case of negative deformations an upsetting of the unidirectionally reinforced undulated yarn is induced due to its undulated shape. In both cases the variation of the amplitude is a superposition of transversal deformation due to Poisson effects as a purely elastic response and a purely kinematic response due to geometric constraints in the mesomechanic scale. In contrast longitudinal deformations applied on a unidirectionally reinforced single layer in direction of the reinforcement leads to a lengthening and shortening in longitudinal direction and a transversal contraction directly coupled due to Poisson effects only.

The repeated acting of this mesomechanic kinematic due to geometric constraints is presumed to enhance the damping properties of fabric reinforced single layers compared to unidirectionally reinforced ones. For an evaluation the free decay behavior of flat beamlike specimens with fabric and unidirectionally reinforced single layers can be considered. Thereby the fixed-free boundary condition has been identified as adequate. During the free decay the structure undergoes the kinematic in a number of cycles equal to the fundamental frequency.

The basic concept and the identification of the acting mechanism has been validated basically in Ottawa et al. 2012 [23] for one set of comparable specimens of basalt fiber reinforced epoxy (0° unidirectionally and 0° twill fabric 2/2 reinforced in warp direction) and more detailed in Romano et al. 2014 [24, 25] and Romano 2016 [26] for three sets of comparable specimens of carbon fiber reinforced epoxy (0° unidirectionally and 0° plain and twill fabric 2/2 reinforced in warp direction).

Thereby, the term comparable is defined by the property and the quality of the composite material of the respective set of specimens. One set of specimens is considered comparable when its single layers consist of the same kind of reinforcement fiber, 0° unidirectionally reinforced on the one hand and 0° fabric reinforced single layers (i. e. in warp direction) on the other hand, with the same polymeric matrix system and additionally at approximately same fiber volume contents $\phi_f = 60\%$ and overall thicknesses of the laminate t .

MESOSCOPIC APPROACH

The phenomena of undulation in fabric reinforced composites are examined on the mesoscopic scale. It is an effect in fabrics as textile semi-finished products. The warp yarns are perpendicularly crossed by the fill yarns alternating at its top and at its bottom. In the following investigations the relatively simple and at the same time easily describable geometry of a balanced plain weave fabric is considered further.

The aim of the carried out investigations is the identification of the previously described acting mesomechanic kinematic correlations. In the carried out analytical and numerical investigations based on plain representative sequences the variable characteristic geometric parameters are the amplitude A and the length of the undulation in the fabric L_F and the length of the cross-section of a roving as a fill yarn L_R , respectively. The parametric variation of the geometric dimensions in realistic steps provides the analysis of the sensitivity of the acting mesomechanic kinematic to the differently shaped undulations.

First a one-dimensional analytic approach is carried out. A kinematic is derived analytically and investigated parametrically. For a first approach strongly simplifying presumptions are necessary, so the elastic parts are neglected in this case.



Parametric FE-calculations allow the consideration of elastic parts. The numerical investigations focus on plain representative sequences as a two-dimensional verification of the analytic model.

Degree of ondulation

In order to definitely describe the differently shaped ondulations regarding the respective intensity of ondulation the specific value \tilde{O} is introduced. The non-dimensional value is based on the afore mentioned characteristic and variable geometric parameters amplitude A and lengths L_F and L_R , respectively. The definition of the degree of ondulation is based on a purely analytical sine

$$y = A \sin\left(2\pi \frac{x}{L}\right) \tag{2}$$

For modeling more sequences in a row it can be repeated in series as often as required, and still yields a continuously differentiable function over the whole domain of definition [27], [28]. For the introduction of the degree of ondulation \tilde{O} the wave steepness S used in nautics, as exemplarily defined in Büsching 2001 [29]

$$S = \frac{H}{L} = \frac{2A}{L} \tag{3}$$

is modified. In Eq. (3) the geometric parameters are the (absolute) wave height $H = 2A$ and the wave length L . In contrast, following the outlook of Ottawa et al. 2012 [23] and the ideas described in Romano et al. 2014 [24, 25] and elaborated in Romano 2016 [26], the degree of ondulation in fabric reinforced plastics is defined by

$$\tilde{O} = \frac{A}{L} = \frac{A}{L_F} = \frac{A}{\lambda L_R} \tag{4}$$

where the geometric parameters are the amplitude A , the lengths of the ondulation in the fabric L_F and the length of the cross-section of a roving as a fill yarn L_R , respectively, and λ is a characteristic factor characterizing the type of the fabric. It is for example $\lambda = 2$ for a plain weave fabric and $\lambda = 4$ for a twill weave 2/2 fabric and can be varied for different fabric constructions. In case of a plain weave fabric it is

$$L_{PL} = \lambda L_R = 2 L_R = L_F \tag{5}$$

Comparison of the structural mechanical motivations

The reason for the modification of the wave steepness S in Eq. (3) to the degree of ondulation \tilde{O} in Eq. (4) is based on the different motivations, necessities and intentions of the respective subject area. In nautics it is important to characterize the absolute load a structure undergoes during its life-cycle, e. g. regarding fatigue strength issues. Therefore, twice the amplitude A corresponding to the absolute wave height H is considered in the calculation of the specific value S [29]. In contrast, when fabric reinforced composites are considered, the characterization of the deviation from the ideally orientated unidirectionally reinforced single layer caused by the ondulation in the fabric is focused. The modification towards considering the single value of the amplitude A can also be interpreted as a degree of eccentricity compared to an unidirectionally reinforced single layer that exhibits an ideally orientated reinforcement without ondulations.

The degree of ondulation \tilde{O} defined in Eq. (4) is a non-dimensional specific value. It corresponds to the rate of intensity of the continuously differentiable geometric direction change of the ondulation. The value enables the comparability of the representative sequences of the analytic model and the ones of the numeric investigations by FE-analyzes. This is at the same time the requirement for the later described verification.

The geometric are chosen in selected and at the same time realistic steps. Whereas the amplitude A is varied from 0.05 mm to 0.25 mm in five substeps of 0.05 mm (0.05 mm; 0.10 mm; 0.15 mm; 0.20 mm; 0.25 mm) the length of the cross-section of a roving as a fill yarn L_R is varied from 2.5 mm to 7.5 mm in five substeps of 1.25 mm (2.5 mm; 3.75 mm; 5.0 mm; 6.25 mm; 7.5 mm). According to Eq. (5) for a plain weave fabric this yields lengths of the ondulation in the fabric L_F from 5.0 mm to 15.0 mm.

The selected values can be considered realistic, as described in detail for the comparable sets of specimens in the experimental validations carried out in Ottawa et al. 2012 [23], Romano et al. 2014 [24, 25] and Romano 2016 [26] or reported by Ballhause 2007 [11], Matsuda et al. 2007 [12] and Kreikmeier et al. 2011 [20].

For a plain weave fabric according to Eq. (5) with $\lambda=2$ and the afore listed geometric parameters yield values of the degree of ondulation \tilde{O} according to Eq. (4) lying in the range of 0.0033 and 0.0500. Fig. 1 right illustrates the degree of ondulation \tilde{O} over a plane spanned by the axes for amplitude A and length of the ondulation in a plain weave fabric L_{PL} with isolines.

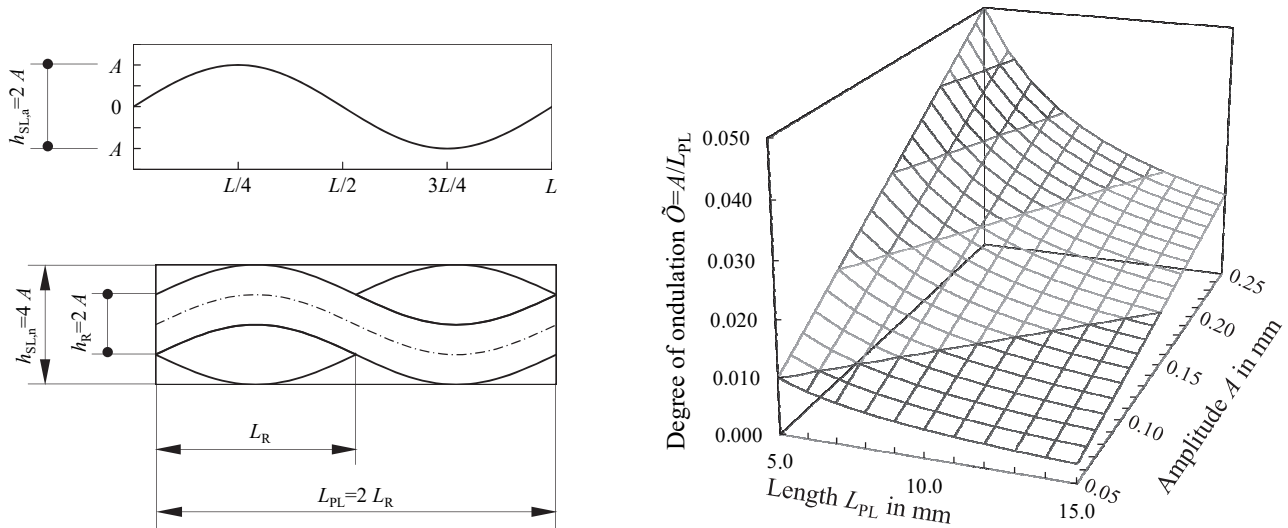


Figure 1: Representative sequences of one complete ondulation based on the characteristic geometric parameters amplitude A and length L of a sine in the analytic model (left top) and for the numerical investigations with FE-calculations (left bottom). Graphical illustration of the degree of ondulation \tilde{O} over a plane spanned by the axes of the geometric parameters amplitude A and length of the ondulation in a plain weave fabric L_{PL} with isolines (right).

ANALYTICAL MODEL AND PROCESSING

The investigations of the purely analytic model are described with its presumptions, processing and evaluation.

Mathematical model and presumptions

The mathematical model for the analytical description of ondulations in fabric reinforced composites reduces the complexity down to a one-dimensional problem. Therefore, only the centerline of an undulated yarn is considered. The obtained mesoscopic geometry is thus an analytical sine. For a representative sequence of one complete ondulation according to Eq. (2) the argument of the sine is presumed in the interval $(2\pi \frac{x}{L}) \in [0, 2\pi]$ that leads to the domain of definition $x \in [0, L]$. The advantages of a trigonometric function are steadiness, differentiability and integrability of its shape on the whole domain of definition [27, 28]. Furthermore the representative domain of definition can be reduced to the wavelength of one complete ondulation, i. e. $D = [0, L]$ because of symmetry properties. With arbitrary amplitude A and $x \in [0, L]$ the representative domain of the argument in the trigonometric function $D = [0, 2\pi]$ is obtained.

In the analytical approach the undulated yarn is assumed not to lengthen or shorten due to strain or compression, but remaining constant in length. Mechanically the presumption of an ideally stiff and at the same time ideally flexible yarn can be stated in terms of an infinite high Young's modulus in longitudinal direction and a negligible flexural modulus transverse to it,

$$E_L = E_1 \rightarrow \infty \quad \text{and} \quad E_T = E_2 \rightarrow 0 \tag{6}$$



The sine shaped yarn further is presumed to be fixed at $x = 0$. The displacements are applied at the zero-crossing $x = L$. A comparable value of deformation due to a displacement in x -direction is the sum of the original length $l_0 = L$ and the applied displacement $\Delta l = l_1 - l_0 = l_1 - L$ referred to the original length by

$$u_{rel} = \frac{\Delta l}{l_0} = \frac{\Delta l}{L} = \frac{l_1 - L}{L} = \frac{l_1}{L} - 1 \quad (7)$$

that is positive for elongation and negative for shortening. The above stated and introduced relation of relative displacements u_{rel} according to Eq. (7) is not a classic elongation or compression that leads to stresses as internal forces, but a geometric deformation due to displacements applied on an ideally stiff and at the same time ideally flexible yarn, indicated by the relations (6) that idealize the qualitative relation (1).

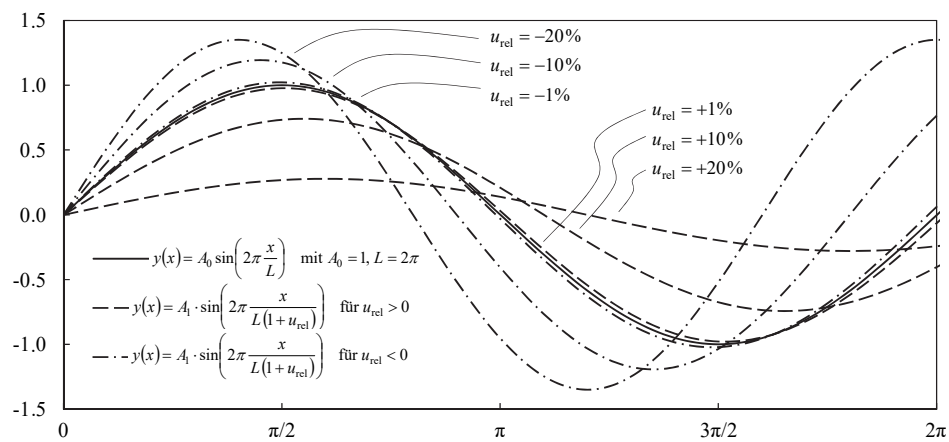


Figure 2: Obtained sines under the presumption of purely geometric deformation of an initial sine with $A_0=1$ and $L=2\pi$: Original graph as bold solid line; Elongated graphs as dashed lines; Shortened graphs as dash-dotted lines.

The applied degrees of deformation u_{rel} (7) have been selected in relevant ranges for structural mechanics of fiber reinforced plastics [10, 30-33]. In detail two decades are considered. The large interval is $u_{rel} = -1 \cdot 10^{-3} \dots +1 \cdot 10^{-3}$ in steps of $1 \cdot 10^{-4}$ and the small interval is $u_{rel} = -1 \cdot 10^{-4} \dots +1 \cdot 10^{-4}$ in steps of $1 \cdot 10^{-5}$. Counting the zero 39 and 21 substeps result for u_{rel} .

The previously stated presumptions lead to two different effects in the model. Positive deformations lead to a smoothing or flattening. The amplitude decreases. In this case the maximum in elongation is reached when the yarn gets completely flattened. In contrast the amplitude increases for a negative deformation applied. In this case the maximum applicable value of the negative deformation is the limit of the domain of definition. Fig. 2 shows the obtained sines under the presumption of purely geometric deformation of an initial sine with an initial amplitude $A_0 = 1$ and domain of the argument $D = [0, 2\pi]$.

Mathematical processing

The arc length of a function is defined by [27, 28]

$$s = \int_0^L \sqrt{1 + (y')^2} dx \quad (8)$$

As carried out in the following, in the case of the presumed sine the solution of Eq. (8) can be achieved by converting it into an elliptic integral of the second kind



$$E(\phi, k) = \int_0^\phi \sqrt{1 - k^2 \sin^2 \phi} \, d\phi \tag{9}$$

For the description of real geometric dimensions the consideration of the arbitrary amplitude A and an arbitrary length L as two independent parameters is necessary. The arc length of a sine can then be achieved by considering the complete elliptic integral of the second kind. Therefore the relation $\sin^2 x + \cos^2 x = 1$ between the squared sine and cosine with the same arguments has to be applied. Additionally, the lower integration limit is set to 0 and the upper integration limit to $\frac{\pi}{2}$, respectively. Carrying out the substitution $\tilde{x} = 2\pi x/L$ one quarter of the arc length can be calculated by

$$\begin{aligned} \frac{1}{4}s &= \int_0^{\frac{\pi}{2}} \sqrt{1 + \left(2\pi \frac{A}{L}\right)^2 \cos^2\left(2\pi \frac{x}{L}\right)} \, dx = \\ &= \int_0^{\frac{\pi}{2}} \sqrt{1 + \left(2\pi \frac{A}{L}\right)^2 \left[1 - \sin^2\left(2\pi \frac{x}{L}\right)\right]} \, dx = \\ &= \int_0^{\frac{\pi}{2}} \sqrt{\left[1 + \left(2\pi \frac{A}{L}\right)^2\right] - \left(2\pi \frac{A}{L}\right)^2 \sin^2\left(2\pi \frac{x}{L}\right)} \, dx = \\ &= \sqrt{1 + \left(2\pi \frac{A}{L}\right)^2} \cdot \int_0^{\frac{\pi}{2}} \sqrt{1 - \frac{\left(2\pi \frac{A}{L}\right)^2}{1 + \left(2\pi \frac{A}{L}\right)^2} \sin^2\left(2\pi \frac{x}{L}\right)} \, dx \end{aligned} \tag{10}$$

The application of the substitution $\tilde{x} = 2\pi x/L$ yields the differential $dx = d\tilde{x}L/(2\pi)$ and leads to

$$\begin{aligned} \frac{1}{4}s &= \sqrt{1 + \left(2\pi \frac{A}{L}\right)^2} \cdot \int_0^{\frac{\pi}{2}} \sqrt{1 - \frac{\left(2\pi \frac{A}{L}\right)^2}{1 + \left(2\pi \frac{A}{L}\right)^2} \sin^2 \tilde{x}} \, d\tilde{x} \cdot \frac{L}{2\pi} = \\ &= \sqrt{\left(\frac{L}{2\pi}\right)^2 + A^2} \cdot \int_0^{\frac{\pi}{2}} \sqrt{1 - \frac{\left(2\pi \frac{A}{L}\right)^2}{1 + \left(2\pi \frac{A}{L}\right)^2} \sin^2 \tilde{x}} \, d\tilde{x} = \\ &= \sqrt{\left(\frac{L}{2\pi}\right)^2 + A^2} \cdot E\left(\frac{\pi}{2}, \sqrt{\frac{\left(2\pi \frac{A}{L}\right)^2}{1 + \left(2\pi \frac{A}{L}\right)^2}}\right) = \\ &= \sqrt{\frac{L^2 + 4\pi^2 A^2}{4\pi^2}} \cdot E\left(\frac{\pi}{2}, \sqrt{\frac{4\pi^2 A^2}{L^2 + 4\pi^2 A^2}}\right) \end{aligned} \tag{11}$$

where the factor $\sqrt{\frac{L^2 + 4\pi^2 A^2}{4\pi^2}}$ can be interpreted as a diminution factor and the argument $\sqrt{\frac{4\pi^2 A^2}{L^2 + 4\pi^2 A^2}}$ can be determined as the elliptic modulus k . The arc length of one complete ondulation s can be calculated by simply multiplying the repeating quarter-sequences with 4 yielding

$$s = \int_0^{2\pi} \sqrt{1 + \left(2\pi \frac{A}{L}\right)^2 \cos^2\left(2\pi \frac{x}{L}\right)} \, dx =$$



$$\begin{aligned}
 &= 4 \cdot \sqrt{\left(\frac{L}{2\pi}\right)^2 + A^2} \cdot \int_0^{\frac{\pi}{2}} \sqrt{1 - \frac{(2\pi A/L)^2}{1 + (2\pi A/L)^2} \sin^2 \tilde{x}} d\tilde{x} = \\
 &= 4 \cdot \sqrt{\left(\frac{L}{2\pi}\right)^2 + A^2} \cdot E \left(\frac{\pi}{2}, \sqrt{\frac{(2\pi A/L)^2}{1 + (2\pi A/L)^2}} \right)
 \end{aligned}
 \tag{12}$$

The previously stated presumptions and boundary conditions have to be fulfilled in order to derive a kinematic due to geometrical constraints only. Therefore the arc length has to remain constant under the application of selected relative displacements u_{rel} . For selected degrees of deformations the governing equation is

$$f(A_1) = s(u_{rel}) - s(u_{rel} = 0) = 0 \tag{13}$$

that is solved numerically in order to determine the resulting root A_1 . For each pre-selected degree of deformation u_{rel} a respective shift in the amplitude ΔA can be calculated according to Eq. (13) by

$$\Delta A = A(u_{rel}) - A(u_{rel} = 0) = A_1 - A_0 \tag{14}$$

that is the shift in amplitude as a function of the applied relative displacements u_{rel} . For further investigations it is reasonable to introduce the relative shift of the amplitude

$$w_{rel} = \frac{\Delta A}{A_0} = \frac{A_1 - A_0}{A_0} = \frac{A_1}{A_0} - 1 \tag{15}$$

in order to receive another relative dimension, corresponding to the relative dimension u_{rel} (7). The relative shift of the amplitude w_{rel} (15) is plotted against the relative displacements u_{rel} (7), and w_{rel} - u_{rel} -diagrams result. The correlation reaches its limit at a degree of deformation

$$u_{rel,max} = \frac{s(A_0) - l_0}{l_0} \tag{16}$$

For this value the algorithm to numerically determine the shift in amplitude reaches a singularity. In this case the singularity represents the state when the former sine gets completely flattened by positive deformation. This leads to an absolute decay of the amplitude A . In contrast shortening as negative deformation shows a less gradient of the shift of the amplitude A towards higher values. In case of applied negative deformations the model under the previously stated presumptions is able to theoretically describe the increase of the amplitude A up to a maximum value in the degree of deformation $u_{rel} = -1$. This state means a complete compression. For this value the algorithm to numerically determine the shift in amplitude exhibits its second singularity.

NUMERICAL INVESTIGATIONS BY FINITE-ELEMENT-ANALYSES

In order to verify the analytical model numerical investigations with the Finite-Element-Analyses (FE-Analyses) are carried out. As linear-elastic FE-calculations are carried out the elastic parts, formerly neglected in the analytical model, are considered. These are namely elasticity and transversal deformation due to Poisson effects of the model under selected longitudinal deformations as strains in terms of relative displacements. In order to identify the originally acting mesomechanic kinematic correlations due to geometric constraints, non-linearities, failure mechanisms and friction effects are neglected. The modeling, setting and processing described in the following is based on the investigations of Ottawa et al. 2012 [23]. Therein different element formulations, number of elements (degree of discretization) and

convergence behavior is considered in sensitivity analyses. The numerical investigations are carried out with the FE-software ANSYS Workbench Version 14.0.1 [34].

FE-model of plain representative sequences

The kinematic is investigated parametrically by varying the characteristic geometric dimensions as well as the boundary conditions. In order to enable a proper meshing, avoid too small or acute triangle elements, reduce computing time and improve convergence two slight but essential modifications of the geometry are necessary.

First, the lens-shaped fill yarns are cut by 2 % regarding the length L_R in the region of each intersection. The resulting length of the cross-section of the fill yarn is $L_{R,mod} = 0.96 \cdot L_R$. The length of the complete plain representative sequence L_{PL} according to Eq. (5) is thereby not affected. Second, the upper and lower horizontal boundary of the surrounding matrix region is increased by 10 % of the amplitude A . The resulting thickness of the modified plain representative sequences is then $t_{mod} = 4.2 \cdot A$. Fig. 3 illustrates the modified parametric model for the numerical investigations by the FE-analyses confronting the extremes of its geometric dimensions.

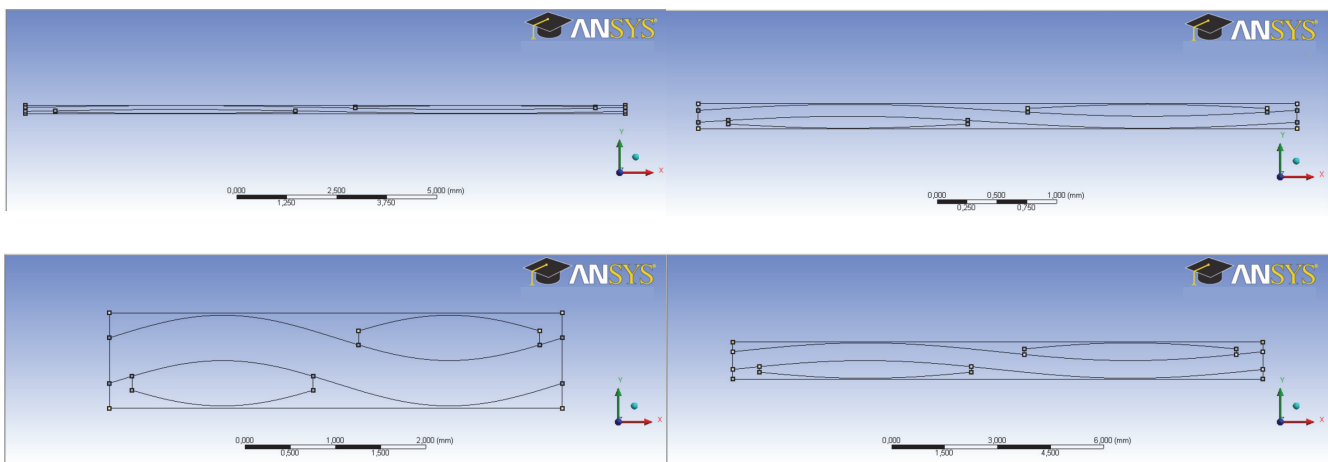


Figure 3: Modified parametric model for investigations by the FEA based on analytic dimensions confronting its extremes. Upper left: Biggest length $L=15$ with lowest amplitude $A=0.05$ yielding $\tilde{\sigma} = 0.00333$; Upper right: Shortest length $L=5$ with lowest amplitude $A=0.05$ yielding $\tilde{\sigma} = 0.01000$; Lower left: Shortest length $L=5$ with highest amplitude $A=0.25$ yielding $\tilde{\sigma} = 0.05000$, Lower right: Biggest length $L=15$ with highest amplitude $A=0.25$ yielding $\tilde{\sigma} = 0.01667$.

FE-settings: Meshing, element types and contact definition

As a first approximation a two dimensional FE-analyses is carried out. The representative sequence is discretized by elements with an average edge length of $1 \cdot 10^{-3}$. As the FE-model represents a cross-section of a structure, a plain strain condition in the x - y -plane is presumed. Plain four-node solid elements with linear shape functions are assigned to each region of the model. An orthotropic material model is chosen for properly applying the material properties to warp and fill yarn.

In case of the region of the warp yarn elements of the formulation PLANE42 are assigned to by APDL (ANSYS Parametric Design Language). In this case the enabled first keyoption by the command KEYOPT(1) for the element formulation PLANE42, makes the local x - y -element coordinate system follow the element I - J sides. As a mapped meshing has been applied to this region, the element coordinate systems follow the sine-shaped undulation. As the material properties of orthotropic materials in ANSYS [34] are orientated along the element coordinate system, the modification is essential for a reality based FE-simulation. To the two other regions (fill yarns and matrix) the default elements of the formulation PLANE182 are retained. It does not provide the afore mentioned keyoption. It neither is necessary because the fill yarns are modeled in their plane of isotropy and the matrix is modeled isotropic. After sensitivity analyses and as a reasonable approach for the real conditions the contact between the single regions is defined by coincident nodes. Fig. 4 illustrates the effect of the different element formulations on the orientation of the element coordinate systems in the region of the zero-crossing.

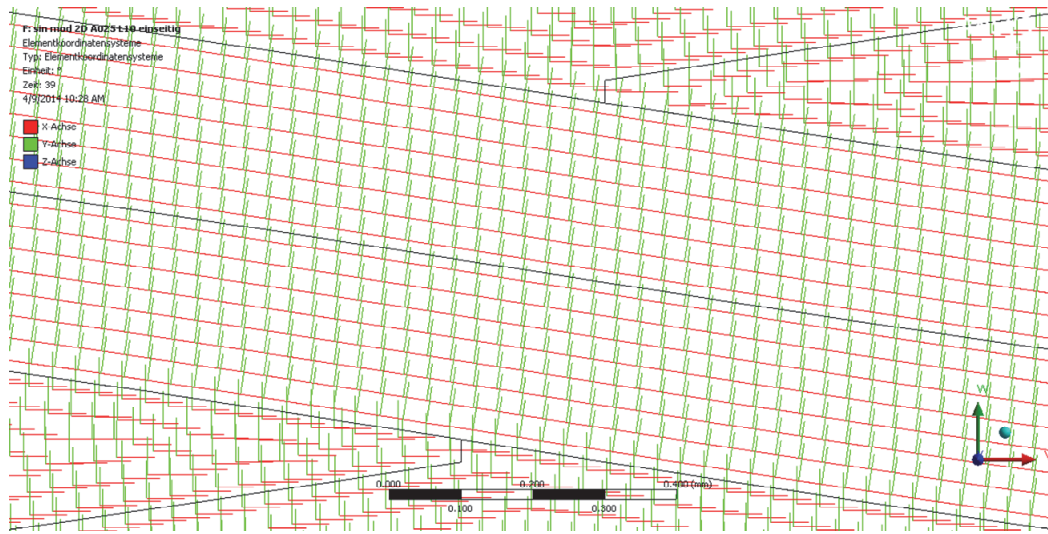


Figure 4: Different element formulations in the region of the zero-crossing: PLANE42 with enabled first keyoption KEYOPT(1) in the region of the ondulated warp yarn causing the element coordinate systems to follow the sine-shaped undulation and PLANE182 in the region of the fill yarns and the matrix with the element coordinate systems aligned to the global coordinate system.

Boundary conditions and application of selected deformations

A clamped edge is defined on one vertical edge. On the opposite vertical edge a free edge is defined where the selected displacements are applied. Both definitions on the boundaries allow a transversal deformation of the cross-section due to Poisson effects, as the translational displacements in the vertical y -direction as well as the rotational degree of freedom to the z -direction perpendicular to the x - y -plane are defined free. On the nodes of the defined free vertical edge selected longitudinal deformations as strains

$$\varepsilon_x = \frac{\Delta l}{l_0} = \frac{u}{L_F} \quad (17)$$

are applied in two intervals. For verification and comparison issues they are the same as used in the analytical model for u_{rel} (7), i. e. the large one is $\varepsilon_x = -1 \cdot 10^{-3} \dots +1 \cdot 10^{-3}$ in steps of $1 \cdot 10^{-4}$ and the small one is $\varepsilon_x = -1 \cdot 10^{-4} \dots +1 \cdot 10^{-4}$ in steps of $1 \cdot 10^{-5}$, resulting in 39 and 21 substeps.

Regarding the boundary conditions on the horizontal edges, i. e. on the top and bottom side of the model, two basically different conditions exist. Fabric reinforced composites usually consist of more than one layer, mostly an even number of plies. Thus the single layers can be considered as elastically supported on both sides, when located as an inner ply, and elastically supported on one side, when located as an outer ply. Therefore, a case-by-case analysis is considered further. The calculation of the value of the elastic support k_{el} is done by means of a weighted average of the plane stiffnesses based on the areas of the different regions. The similar calculation is carried out by Barbero 2011 [35], 2006 [10] and 1995 [36] as well as by Byun 2000 [4].

Structural mechanic material properties of the single components

The two exemplarily considered single components are HT-carbon fibers as reinforcement fibers and epoxy resin as a polymeric matrix system. Because of its characteristic structural mechanic material properties this combination is commonly used in mechanically highly loaded structures. Tab. 1 contains the structural mechanic material properties the two components, taken from [30-33]. The densities of the single components as a physical material property are indicated for the HT-carbon fibers $\rho_{HT-Carbon} = 1.74 \text{ g/cm}^3$ and for the epoxy resin as matrix system $\rho_m = 1.20 \text{ g/cm}^3$. In detail the structural mechanic material properties correspond to the values indicated in the data sheets of the three sets of comparable specimens of HT-carbon fiber reinforced epoxy, used in the experimental investigations described in Romano et al. 2014 [24, 25] and Romano 2016 [26].



Reinforcement fibers <i>Structural mechanic material property</i>	HT-Carbon <i>Value</i>	Polymeric matrix <i>Structural mechanic material property</i>	Epoxy resin <i>Value</i>
Young's modulus $E_{f,1}$	230 GPa	Young's modulus E_m	3.3 GPa
Young's modulus $E_{f,2}$	28 GPa	Shear modulus G_m^*	1.22 GPa*
Shear modulus $G_{f,12}$	50 GPa	Poisson's ratio ν_m	0.35
Shear modulus $G_{f,23}^*$	11.4 GPa*		
Poisson's ratio $\nu_{f,12}$	0.230		
Poisson's ratio $\nu_{f,21}^{**}$	0.028**		
Poisson's ratio $\nu_{f,23}$	0.225		

* no independent structural mechanic material property, determined because of presumed (quasi-)isotropy
 ** no independent structural mechanic material property, determined by relation according to Maxwell-Betti

Table 1: Structural mechanic material properties of the single components according to [30-33]: Left: HT-carbon as reinforcement fibers. Right: Epoxy resin as polymeric thermoset matrix system.

<i>Region of plane rep. sequence</i>	Kind of fiber reinforcement:		
	<i>Longitudinally cut (warp yarn)</i>	HT-carbon fiber reinforced epoxy	
		<i>Micromechanic homogenization</i>	<i>Transversally cut (fill yarn)</i>
Young's modulus E_1	150.7 GPa	weighted average stiff	11.4 GPa
Young's modulus E_2	11.4 GPa	Chamis 1983/84 [37], [38]	11.4 GPa
Young's modulus E_3	11.4 GPa	Chamis 1983/84 [37], [38]	150.7 GPa
Shear modulus G_{12}	5.7 GPa	Chamis 1983/84 [37], [38]	3.7 GPa*
Shear modulus G_{23}	3,7 GPa*	Tsai 1980 [39]	5.7 GPa
Shear modulus G_{13}	5.7 GPa	Chamis 1983/84 [37], [38]	5.7 GPa
Poisson's ratio ν_{12}	0.272	weighted average Poisson	0.333
Poisson's ratio ν_{23}	0.333	Foye 1972 [40]	0.021*
Poisson's ratio ν_{13}	0.272	weighted average Poisson	0.021*

* no independent structural mechanic material property for transversally isotropic material behavior

Table 2: Homogenized structural mechanic material properties of the 0°-unidirectionally reinforced single layer of HT-carbon fiber reinforced epoxy resin in the local 1-2-3-coordinate system of the respective region of the warp and fill yarn at the presumed fiber volume content of $\phi_{f,r} = 65\%$ as the input values for the input mask of the FE-preprocessor of ANSYS [34]

Homogenized structural mechanic material properties of the 0°-unidirectionally reinforced single layer

The fiber reinforced regions (warp and fill yarns) are considered as 0°-unidirectionally reinforced, having the same (local) fiber volume content. Because of the transversally isotropic material behavior to the fiber direction, there are five independent structural mechanic material properties in the local 1-2-3-coordinate system.

Tab. 2 contains the homogenized structural mechanic material properties of the 0°-unidirectionally reinforced single layer of HT-carbon fiber reinforced epoxy resin in the local 1-2-3-coordinate system of the respective region of the warp and fill yarn. Thereby, an achievable and technically reasonable local fiber volume content of $\phi_{f,r} = 65\%$ is presumed. The applied rules of mixtures are referenced. The density of the composite material ρ_c is calculated as a weighted average of the densities of the single components based on the fiber volume content. The physical material property for HT-carbon fiber reinforced epoxy at $\phi_{f,r} = 65\%$ is $\rho_{c,HT-Carbon-EP} = 1.55 \text{ g/cm}^3$.



Assignment of the structural mechanic material properties to the different region

The assignment of the structural mechanic material properties to the different region follows according to the respective input mask of the FE-preprocessor of ANSYS [34].

For the HT-carbon fiber reinforced regions the input mask of an orthotropic material behavior is used. For a complete and consistent FE-simulation the input of 3D-properties are required, although 2D-properties are applied due to the carried out 2D-analyses. Nine independent structural mechanic material properties are required. Yet, the five independent values of the 0°-unidirectionally reinforced regions suffice, as pairwise equal inputs are made in the plane of isotropy for simulation of transversal isotropic material behavior. Tab. 2 contains the input values of the structural mechanic material properties of the fiber reinforced regions.

To the regions of pure matrix without fiber reinforcement are assigned the isotropic material properties $E_m = 3,3$ GPa and $\nu_m = 0.35$ as indicated in Tab. 1. According to the case-by-case analysis, considering the two basically different boundary conditions, the elastic support $k_{el,HT-carbon-EP} \approx 9.5$ GPa acting in transversal y -direction of the FE-model is assigned to. The detailed calculation of the value of the elastic support, by the weighted average of the perpendicular stiffnesses E_2 and E_m in the plane of the representative sequence, based on the relative part of the areas of the different regions, is carried out according to Barbero 2006 [10], 2011 [35] and 1995 [36] as well as to Byun 2000 [4].

RESULTS AND DISCUSSION

The obtained results of both the analytical model and the numerical investigations by the FE-analyses are evaluated and compared to each other. The acting mechanisms of the mesomechanic kinematic in fabrics due to the degree of ondulation and its sensitivity to geometric parameters and boundary conditions are described and discussed.

Aspects of the evaluation

The variation of the two characteristic geometric dimensions of the ondulation in five substeps each provides 25 combinations of different degrees of ondulation \tilde{O} in total. For each of the models, the same selected deformations are applied in two decades of ten equidistant steps each. The relevant results are evaluated for every degree of ondulation \tilde{O} at every substep $n = 0, \dots, 39$ and plotted against the selected deformations. These are u_{rel} (7) in the analytical model and ϵ_x in the numerical investigations (17).

Positions of evaluation and separation of elastic and kinematic parts

The relevant positions of evaluation of the analytical model correspond to the ones of the FE-model. In case of the plain representative sequence of a plain weave fabric they are the two extrema, namely maximum and minimum of the sine. In case of the numerical investigations these are located on the theoretical center-line of the longitudinally cut ondulated warp yarn. The evaluation of the results is carried out by the linearly presumed correlation between the applied displacements and the considered relevant values, analog to Ottawa et al. 2012 [23]. In the FE-calculations the resulting elastic deformation basically consists of two parts. These consist of the purely kinematic parts due to geometric constraints and of the resulting elastic behavior of the linear-elastically modeled material. In order to identify the kinematic part only, the elastic part has to be separated from the total deformation.

Sensitivity to the mesomechanic kinematic

In each case almost linear correlations can be identified, especially in the smaller interval. A direct and linear coupling between deformation and shape of the ondulation in fabric reinforced single layers can be stated, and the absolute value of the negative slope

$$\begin{aligned} \tilde{M}_{y,a}(\tilde{O}) &= \frac{dw_{rel}}{du_{rel}} \text{ in case of the analytical model and} \\ \tilde{M}_y(\tilde{O}) &= \frac{d\epsilon_{y,kin}}{d\epsilon_x} \text{ and } \tilde{M}_x(\tilde{O}) = \frac{d\epsilon_{x,kin}}{d\epsilon_x} \text{ in case of the numerical model} \end{aligned} \tag{18}$$

as a function of the degree of ondulation \tilde{O} represents the sensitivity to the mesomechanic kinematic. With the definition of the slopes \tilde{M} (18) another relative value is introduced. Thereby, a higher slope \tilde{M} or a higher absolute value of it



$|\tilde{M}|$ corresponds to a higher sensitivity to the mesomechanic kinematic, whereas a smaller value implies a smaller one. In the following the sign sensitive values of the slopes \tilde{M} are considered.

Results

The results are presented in terms of the transversal kinematic part and in the difference of the applied and the evaluated longitudinal deformation.

Transversal kinematic part

The displacements v in transversal direction as y -displacements v are evaluated by the difference of the values v_1 and v_2 , where the indices indicate the opposite relevant positions. Because the FE-calculations consider the elastic part, the relative shift of the amplitude is lead back to the total transversal deformation (y -strain ε_y). This value results as the ratio of the difference of the y -displacements Δv to the originally perpendicular distance of the positions of evaluation to each other. It is twice the amplitude, i. e. $2A$, for every mesomechanic geometry. The total transversal deformation for every substep $n = 1, \dots, 39$ is

$$\varepsilon_{y,n,tot} = \frac{\Delta v}{2A} = \frac{v_{1,n} - v_{2,n}}{2A} \quad (19)$$

It is the sum of the purely kinematic part due to geometric constraints $\varepsilon_{y,kin}$ and the transversal strain due to Poisson effects $\varepsilon_{y,PRS}$ of the plain representative sequence. The results of Eq. (19) have to be corrected by the transversal deformation due to Poisson effects. Solved for the kinematic part due to mesomechanic geometric constraints it is

$$\varepsilon_{y,n,kin} = \varepsilon_{y,n,tot} - \varepsilon_{y,n,PRS} = \frac{v_{1,n} - v_{2,n}}{2A} - \varepsilon_{y,n,PRS} \quad (20)$$

where the transversal deformation due to Poisson effects of the sequence is determined by

$$\varepsilon_{y,n,PRS} = -\nu_{PRS,12} \varepsilon_{x,n} = -\nu_{PRS,12} \varepsilon \quad (21)$$

It is defined as the negative relation of transversal deformation due to the longitudinal one (cf. Eq. (17)). The value of the plain representative sequence $\nu_{PRS,12}$, used in Eq. (21), is calculated by the weighted average of the Poisson's ratios of the three structural mechanic different regions based on its areas of the sequence A . For simplification, for the longitudinally cut warp yarn the value of a 0° -unidirectionally reinforced region ν_{12} is presumed, despite of its ondulation. For the perpendicularly cut transversal isotropic fill yarns the value is the one of the plane of isotropy, i. e. ν_{23} , and the Poisson's ratio of the isotropic matrix is ν_m . Thus, the Poisson's ratio of the plain representative sequence follows by

$$\nu_{PRS,12} = \frac{A_W}{A_{PRS}} \nu_{12} + \frac{A_F}{A_{PRS}} \nu_{23} + \frac{A_M}{A_{PRS}} \nu_m \quad (22)$$

In case of the values of the HT-carbon fiber reinforced epoxy, namely $\nu_{12} = 0.272$, $\nu_{23} = 0.333$ and $\nu_m = 0.35$, as indicated in Tab. 1 and Tab. 2, Eq. (22) yields $\nu_{PRS,12} \approx 0.306$ as the value of the Poisson's ratio of the representative sequence.

Difference of the applied and the evaluated longitudinal deformation

An additional indicator for the acting of the mesomechanic kinematic due to geometric constraints is the difference of the applied and the evaluated deformations in longitudinal direction (x -direction) $\Delta \varepsilon_x = \varepsilon_{x,kin}$. The difference of the applied



deformations $\epsilon_{x,n}$ (17) and the evaluated or calculated ones by FE-analyzes in longitudinal direction at the relevant positions $\epsilon_{x,n,FE}$ for every substep $n = 1, \dots, 39$ is

$$\epsilon_{x,n,kin} = \Delta\epsilon_{x,n} = \epsilon_{x,n} - \epsilon_{x,n,FE} \tag{23}$$

It serves for the identification of the elastic deformation of the plain representative sequence and the longitudinally cut undulated warp yarn in the FE-model.

Results of the analytical model

Tab. 3 lists the evaluated results according to Eq. (18) in the $w_{rel}-u_{rel}$ -diagram as absolute values $|\tilde{M}_{y,a}|$ over the selected degrees of ondulation \tilde{O} of the analytical model. The results are listed in ascending order regarding the corresponding degree of ondulation \tilde{O} . Fig. 5 graphically illustrates the correlations of the selected degrees of ondulation and the corresponding sensitivity to the mesomechanic kinematic. The consideration of the absolute values of the slopes in the $w_{rel}-u_{rel}$ -diagram $|\tilde{M}_{y,a}|$ allows a graphical illustration of the correlation between degree of ondulation \tilde{O} and the sensitivity to the mesomechanic kinematic in a linear equidistant scaled diagram and in a double logarithmic scaled diagram. In both cases the results are illustrated separately for the large and for the small interval, and the equations of a hyperbolic approximation of the correlation for the respective interval are indicated. Additionally, the upper bound that can be identified for the exponent -1.5 is visualized by a bold dashed line.

Geometric parameters of the ondulation			Slope $ \tilde{M}_{y,a} $ in the $w_{rel}-u_{rel}$ -diagram	
Amplitude A	Length of ondulation L	Degree of ondulation \tilde{O}	Analytically for $u_{rel} = \mp 1 \cdot 10^{-3}$ in steps of $1 \cdot 10^{-4}$	Analytically for $u_{rel} = \mp 1 \cdot 10^{-4}$ in steps of $1 \cdot 10^{-5}$
0.05	15.0	0.00333	-2448.20	-5040.10
0.05	12.5	0.00400	-1886.70	-3288.40
0.05	10.0	0.00500	-1369.90	-2047.40
0.10	15.0	0.00667	-914.03	-1143.40
0.05	7.5	0.00667	-914.59	-1141.30
0.10	12.5	0.00800	-729.59	-793.20
0.15	15.0	0.01000	-540.08	-507.26
0.10	10.0	0.01000	-540.13	-507.13
0.05	5.0	0.01000	-540.14	-505.79
0.15	12.5	0.01200	-369.62	-352.36
0.20	15.0	0.01333	-293.84	-285.42
0.10	7.5	0.01333	-293.67	-285.23
0.15	10.0	0.01500	-229.49	-225.43
0.20	12.5	0.01600	-200.78	-198.17
0.25	15.0	0.01667	-184.74	-182.66
0.25	12.5	0.02000	-127.63	-126.94
0.20	10.0	0.02000	-127.54	-126.90
0.15	7.5	0.02000	-127.64	-126.92
0.10	5.0	0.02000	-127.50	-126.90
0.25	10.0	0.02500	-81.45	-81.28
0.20	7.5	0.02667	-71.61	-71.49
0.15	5.0	0.03000	-56.60	-56.54
0.25	7.5	0.03333	-45.86	-45.83
0.20	5.0	0.04000	-31.92	-31.91
0.25	5.0	0.05000	-20.50	-20.50

Table 3: Slopes in the $w_{rel}-u_{rel}$ -diagram, i. e. $|\tilde{M}_{y,a}|$ of the selected degrees of ondulation \tilde{O} for the two considered intervals of u_{rel} .

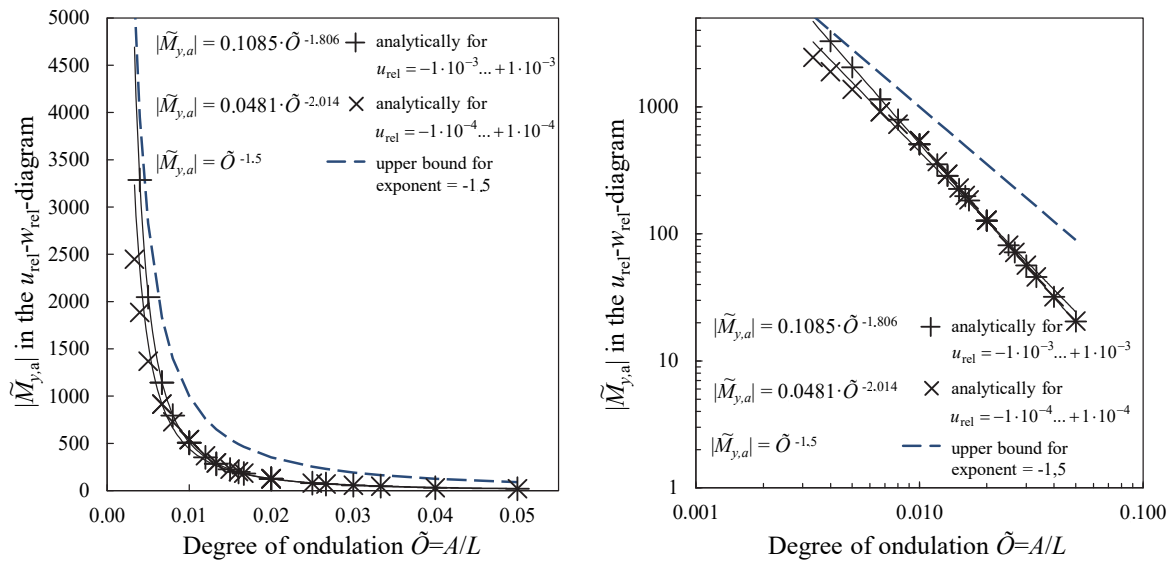


Figure 5: Absolute values of the slopes, i. e. $|\tilde{M}_{y,a}|$, over the selected degrees of ondulation \tilde{O} plotted against the selected degrees of ondulation \tilde{O} in a linear equidistant scale (left) and in a double logarithmic scale (right).

Results of the FE-calculations

In case of the two-sided elastic support the opposed positions of evaluation in the transversal direction (y -direction) behave symmetrically and contrary identical, because of the symmetry of the model and the boundary conditions. In contrast in case of the one-sided elastic support the free position behaves distinctly more sensitive as the supported position. The consideration of the longitudinal direction (x -direction) in both cases of the elastic support the evaluated results behave identically. Thereby the evaluation of Eq. (20) and Eq. (23) yields causally determined comprehensible and significant correlations.

The evaluated results over the degree of ondulation \tilde{O} for the applied deformations ε_x of the numerical model are listed in Tab. 4 for the kinematic parts $\varepsilon_{y,kin}$ (20) in terms of the slopes \tilde{M}_y , and in Tab. 5 for the difference of the applied and evaluated longitudinal deformation $\varepsilon_{x,kin}$ (23) in terms of the slopes \tilde{M}_x . The results are graphically illustrated in Fig. 6 and Fig. 7, respectively. With an increasing degree of ondulation \tilde{O} the results show an increasing sensitivity in terms of the absolute values of the slopes \tilde{M} . In case of the kinematic parts $\varepsilon_{y,kin}$ (20) it is possible to imply a sigmoidal correlation. The case of the one-sided elastic support shows a 1.8 times higher sensitivity to the mesomechanic kinematic as the case of the two-sided one. In case of the difference of the applied and evaluated longitudinal deformation $\varepsilon_{x,kin}$ it is possible to imply a quadratic correlation, where the one-sided elastic support shows again a higher sensitivity as the two-sided one.

Discussion

Due to its geometric similarity the results of the analytical model and of the numerical investigations of the plain weave fabric are comparable to each other, although they are partially identified by strongly simplifying presumptions. However both provide a description of the kinematic behavior by trend.

The elastic parts of the ondulated roving due to the applied deformation are not negligible. Additionally, it has a certain bending stiffness due to its extent in the direction of the thickness. Both effects are considered by the numerical investigations with the FE-calculations. Furthermore the difference of the structural mechanic behavior of fiber reinforced plastics under tensile and compression load, the quality of the inter- and intralaminar adhesion between the single components (interphase) or the single layers (interlaminar shear stiffness) or other damages as imperfections, influence the real material behavior.

Aspects considered in previously published contributions regarding mesomechanic kinematic correlations in fabric reinforced plastics are generally non-linear, especially when the kinematic correlations for dry fabrics without matrix system under uniaxial and biaxial loading as well as under shear loading are considered [11, 14, 15, 18]. Thereby at high rates of positive deformations the smoothing or flattening of the loaded yarns causes an upsetting of the transversally

orientated yarns. This mechanism results in an increase of the thickness of the fabric instead of a decrease of the thickness.

Geometric parameters of the ondulation			Slope \tilde{M}_y in the $\varepsilon_{y,kin} - \varepsilon_x$ -diagram	
Amplitude A	Length of ondulation L	Degree of ondulation \tilde{O}	CFRP one-sided elastically supported	CFRP two-sided elastically supported
0.05	15.0	0.00333	-0.3180	-0.1588
0.05	12.5	0.00400	-0.4301	-0.2156
0.05	10.0	0.00500	-0.6451	-0.3260
0.10	15.0	0.00667	-0.5985	-0.2714
0.05	7.5	0.00667	-1.0954	-0.5525
0.10	12.5	0.00800	-0.8398	-0.3902
0.15	15.0	0.01000	-0.9322	-0.4124
0.10	10.0	0.01000	-1.2895	-0.6098
0.05	5.0	0.01000	-2.3964	-1.1946
0.15	12.5	0.01200	-1.3223	-0.6001
0.20	15.0	0.01333	-1.3044	-0.5711
0.10	7.5	0.01333	-2.2863	-1.1021
0.15	10.0	0.01500	-2.0499	-0.9564
0.20	12.5	0.01600	-1.8562	-0.8374
0.25	15.0	0.01667	-1.6981	-0.7333
0.25	12.5	0.02000	-2.4066	-1.1001
0.20	10.0	0.02000	-2.8025	-1.3188
0.15	7.5	0.02000	-3.4763	-1.7109
0.10	5.0	0.02000	-4.7204	-2.4144
0.25	10.0	0.02500	-3.4963	-1.6928
0.20	7.5	0.02667	-4.4191	-2.2506
0.15	5.0	0.03000	-6.0830	-3.3707
0.25	7.5	0.03333	-5.0427	-2.6973
0.20	5.0	0.04000	-6.4358	-3.8950
0.25	5.0	0.05000	-6.1304	-4.0234

Table 4: Slopes in the $\varepsilon_{y,kin} - \varepsilon_x$ -diagram \tilde{M}_y for the selected degrees of ondulation \tilde{O} .

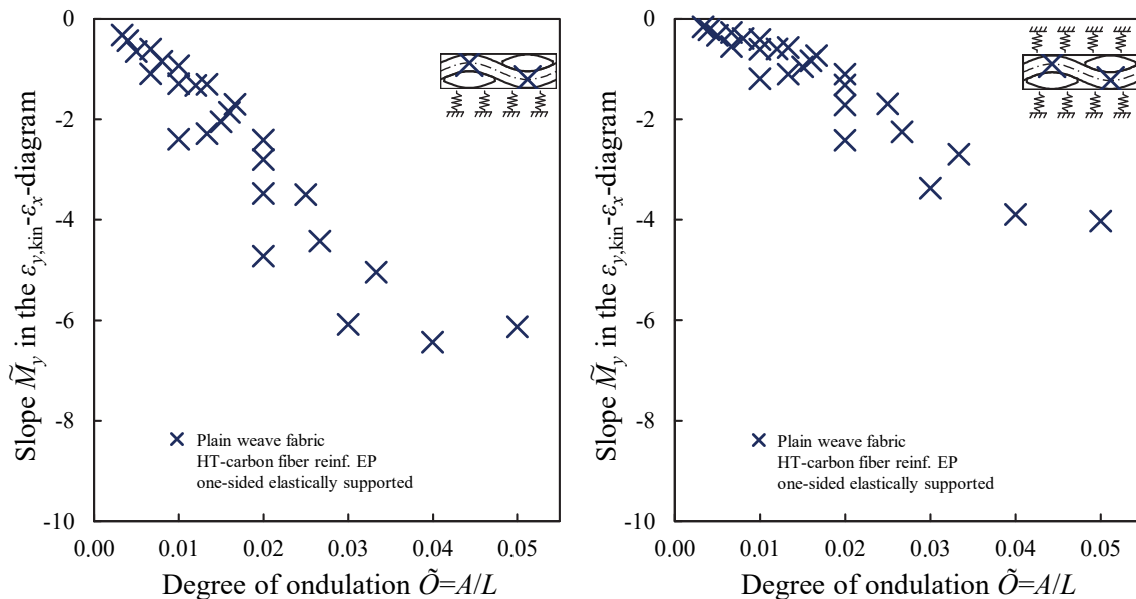


Figure 6: Slopes in the $\varepsilon_{y,kin} - \varepsilon_x$ -diagram \tilde{M}_y plotted over the selected degrees of ondulation \tilde{O} .



Geometric parameters of the ondulation			Slope \tilde{M}_x in the $\varepsilon_{x,kin} - \varepsilon_x$ -diagram	
Amplitude A	Length of ondulation L	Degree of ondulation \tilde{O}	CFRP one-sided elastically supported	CFRP two-sided elastically supported
0.05	15.0	0.00333	0.0182	0.0172
0.10	15.0	0.00400	0.0170	0.0162
0.15	15.0	0.00500	0.0189	0.0177
0.20	15.0	0.00667	0.0184	0.0182
0.25	15.0	0.00667	0.0196	0.0186
0.05	12.5	0.00800	0.0189	0.0193
0.10	12.5	0.01000	0.0203	0.0207
0.15	12.5	0.01000	0.0211	0.0212
0.20	12.5	0.01000	0.0241	0.0224
0.25	12.5	0.01200	0.0232	0.0234
0.05	10.0	0.01333	0.0248	0.0248
0.10	10.0	0.01333	0.0286	0.0275
0.15	10.0	0.01500	0.0308	0.0300
0.20	10.0	0.01600	0.0321	0.0309
0.25	10.0	0.01667	0.0324	0.0326
0.05	7.5	0.02000	0.0464	0.0432
0.10	7.5	0.02000	0.0501	0.0463
0.15	7.5	0.02000	0.0559	0.0483
0.20	7.5	0.02000	0.0666	0.0554
0.25	7.5	0.02500	0.0797	0.0690
0.05	5.0	0.02667	0.1026	0.0865
0.10	5.0	0.03000	0.1560	0.1257
0.15	5.0	0.03333	0.1683	0.1392
0.20	5.0	0.04000	0.2746	0.2254
0.25	5.0	0.05000	0.3917	0.3333

Table 5: Slopes in the $\varepsilon_{x,kin} - \varepsilon_x$ -diagram \tilde{M}_x for the selected degrees of ondulation \tilde{O} .

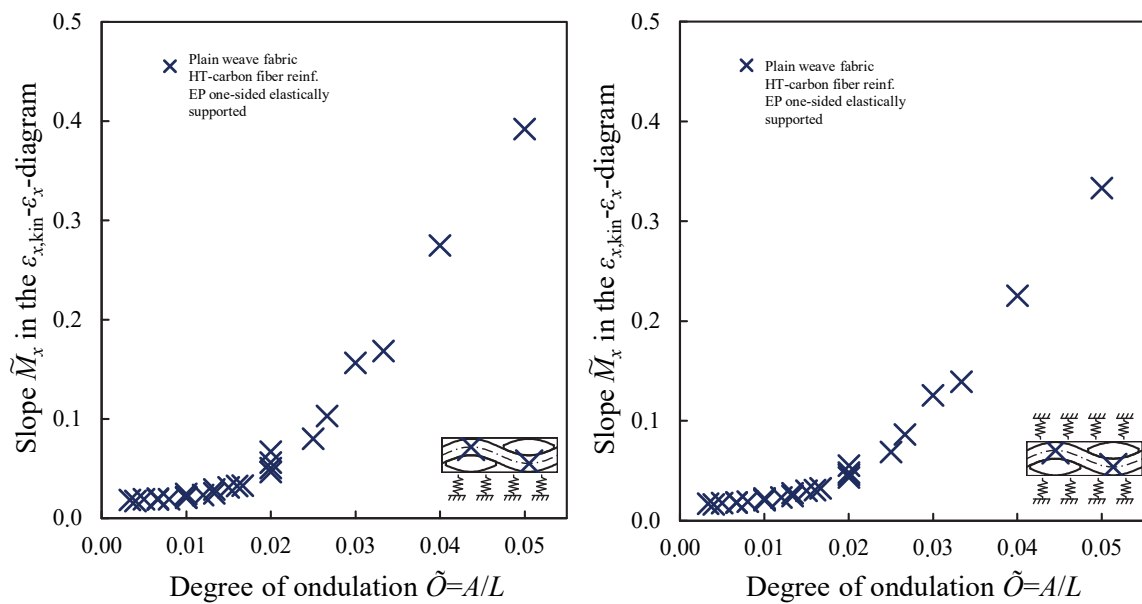


Figure 7: Slopes in the $\varepsilon_{x,kin} - \varepsilon_x$ -diagram \tilde{M}_x plotted over the selected degrees of ondulation \tilde{O} .

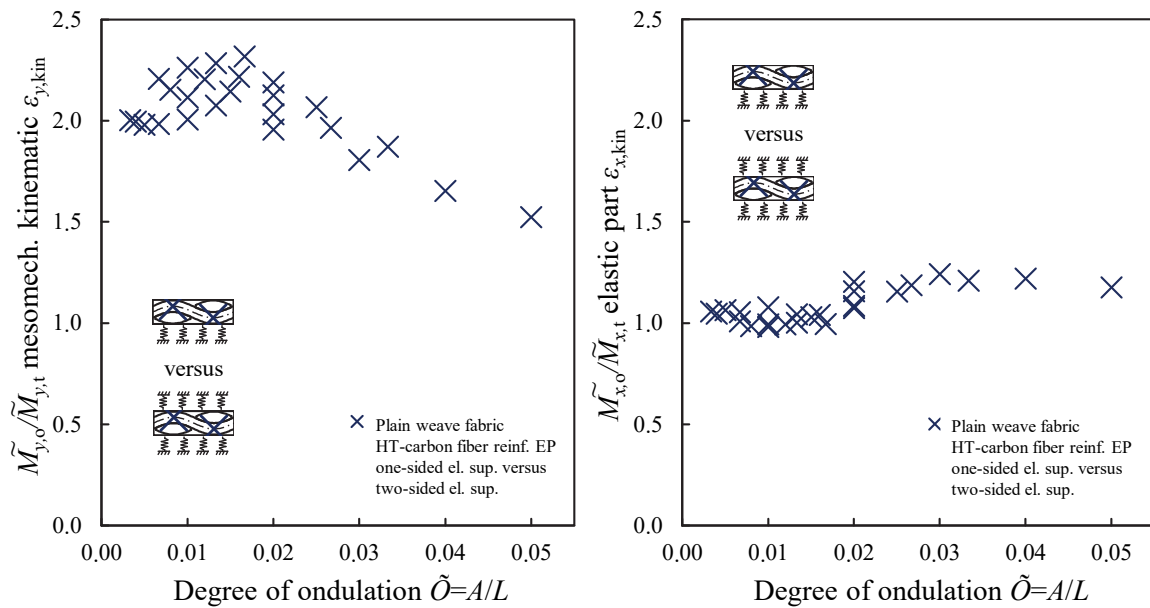


Figure 8: Relations of the sensitivity of the mesomechanic kinematic of the model with one-sided elastic support to the one of two-sided elastic support for the kinematic part (left) and for the difference of the longitudinal deformation (right).

The relations of the sensitivity of the values of the slopes \tilde{M}_y over the degree of ondulation \tilde{O} for the applied deformations ε_x for a balanced plain weave fabric construction of HT-carbon fiber reinforced epoxy are illustrated in Fig. 8, left for the kinematic parts $\varepsilon_{y,kin}$ (20) and right for the difference of the applied and evaluated longitudinal deformation $\varepsilon_{x,kin}$ (23). In case of the kinematic parts $\varepsilon_{y,kin}$ (20) the model with a one-sided elastic support shows a 1.8 times higher sensitivity as the model with a two-sided one. In case of the difference of the applied and evaluated longitudinal deformation $\varepsilon_{x,kin}$ (23) the model with a one-sided elastic support only slightly differs from the model with a two-sided elastic one. Correspondingly the relation of the sensitivities $\tilde{M}_{x,o} / \tilde{M}_{x,t}$ plotted over the degrees of ondulation \tilde{O} is almost constant about approximately 1.

CONCLUSIONS

The identified correlations in the analytical and numerical investigations definitely prove and verify the acting of a mesomechanic kinematic due to geometric constraints. Within the limits of the validity of the analytical and numerical model a direct linear coupling between the applied longitudinal deformations and the mesomechanic kinematic exists. In case of the FE-calculations the transversal deformation due to Poisson effects as an elastic reaction is separated and corrected, in order to obtain the purely mesomechanic kinematic. Yet, the simplifying presumptions of the analytical model are suitable only to describe the tendency of the kinematic behavior, because the idealized stiffnesses only qualitatively represent the huge differences of the stiffnesses in the direction of the fibers and transverse to it.

In order to obtain more precise results, more parameters, especially in the FE-calculations, can be varied in further investigations. Considering plain representative sequences, amongst others, correlations regarding loading and displacements or deformations as well as detailed analyses of the resulting stress condition are relevant. A parameter identification of the mesomechanic kinematic regarding the resulting correlations of load and displacement provides the basis for the identification of the influence of the kind of reinforcement fiber (glass, aramid, basalt compared to carbon) and of the kind of fabric construction (twill weave, satin weave (balanced and unbalanced) compared to plain weave) on the structural mesomechanic material behavior of fabrics. Detailed analyses of the stress conditions allow the description of damage mechanisms and the formulation of failure criteria. The consideration of a linear visco-elastic material model instead of a linear-elastic material model, and the consideration of the sensitivity of the material behavior on the kind of deformation (tension or compression) provide another expansion of the limits of the model conceptions. The expansion



of the model to the third direction as the width of the (laminated) load bearing structures, so that representative volume elements (RVEs) instead of plain representative sequences (PRS) are considered, provides a further extension for the consideration of surface structures.

REFERENCES

- [1] Naik, N. K., Shembekar, P. S., Elastic Behavior of Woven Fabric Composites: I-Lamina Analysis, *Journal of Composite Materials*, 26/15 (1992) 2196-2225. DOI:10.1177/002199839202601502
- [2] Mital, S. K., Murthy, L. N., Chamis, C. C., Simplified Micromechanics of Plain Weave Composites, *NASA Technical Memorandum 107165*, (1996) 1-12.
- [3] Guan, H., Micromechanical analysis of viscoelastic damping in woven fabric-reinforced polymer matrix composites, Wayne State University, Detroit, AAI9725829 (1997).
<http://digitalcommons.wayne.edu/dissertations/AAI9725829>.
- [4] Byun, J.-H., The analytical characterization of 2-D braided textile composites, *Composites Science and Technology*, 60(5) (2000) 705-716.
- [5] Huang, Z. M., The mechanical properties of composites reinforced with woven and braided fabrics, *Composites Science and Technology*, 60(4) (2000) 479-498.
- [6] Guan, H., Gibson, R.F., Micromechanic Models for Damping in Woven Fabric-Reinforced Polymer Matrix Composites, *Journal of Composite Materials*, 35(16) (2001) 1417-1434.
- [7] Tabiei, A., Yi, W., Comparative study of predictive methods for woven fabric composite elastic properties, *Composite Structures*, 58(1) (2002) 149-164. DOI:10.1016/S0263-8223(02)00028-4
- [8] Le Page, B. H., Guild, F. J., Ogin, S. L., Smith, P. A., Finite element simulation of woven fabric composites, *Composites Part A*, 35/7-8 (2004) 861-872. DOI:10.1016/j.compositesa.2004.01.017
- [9] Wielage, B., Müller, T., Lampke, T., Richter, U., Kieselstein, E., Leonhardt, G., Simulation der elastischen Eigenschaften gewebeverstärkter Verbundwerkstoffe unter Berücksichtigung der Mikrostruktur, in: M. Schlimmer (Ed.), *Proceedings of the 15. Symposium Verbundwerkstoffe und Werkstoffverbunde*, Kassel, Wiley VCH Verlag, Weinheim, (2005) 441-446. http://www.dgm.de/download/tg/706/706_77.pdf
- [10] Barbero, E. J., Trovillion, J., Mayugo, J. A., Sikkil, K. K., Finite Element Modeling of Plain Weave Fabrics from Photomicrograph Measurements, *Composite Structures*, 73(1) (2006) 41-52.
- [11] Ballhause, D., Diskrete Modellierung des Verformungs- und Versagensverhaltens von Gewebemembranen, University of Stuttgart, Stuttgart, (2007).
- [12] Matsuda, T., Nimiya, Y., Ohno N., Tokuda M., Elastic-viscoplastic behavior of plain-woven GFRP laminates: Homogenization using a reduced domain of analysis, *Composite Structures*, 79 (2007) 493-500.
- [13] Nakanishi, Y., Matsumoto, K., Zako, M., Yamada, Y., Finite element analysis of vibration damping for woven fabric composites, *Key Engineering Materials*, 334-335 (2007) 213-216.
- [14] Badel, P., Vidal-Sallé, E., Boisse, P., Computational determination of in-plane shear mechanic behaviour of textile composite reinforcements, *Computational Material Science*, 40 (2007) 439-448.
- [15] Hivet, G., Boisse, P., Consistent mesoscopic mechanical behavior model for woven composite reinforcements in biaxial tension, *Composites Part B*, 39 (2008) 345-361.
- [16] El Mahi, A., Assarar, M., Sefrani, Y., Berthelot, J.-M., Damping analysis of orthotropic composite materials and laminates, *Composites Part B*, 39 (2008) 1069-1076.
- [17] Szablewski, P., Sinusoidal Model of Fiber-reinforced Plastic Composite, *Journal of Industrial Textiles*, 38(4) (2009) 277-288. DOI: 10.1177/1528083708098914.
- [18] Hivet, G., Duong, A.V., A contribution to the analysis of the intrinsic shear behavior of fabrics, *Journal of Composite Materials*, 45(6) (2010) 695-716.
- [19] Ansar, M., Xinwei, W., Chouwei, Z., Modeling strategies of 3D woven composites, A review, *Composite Structures*, 93 (2011) 1947-1963.
- [20] Kreikmeier, J., Chrupalla, D., Khattab, I. A., Krause, D., Experimentelle und numerische Untersuchungen von CFK mit herstellungsbedingten Fehlstellen, *Proceedings of the 10. Magdeburger Maschinenbau-Tage*, Magdeburg, (2011).
- [21] Valentino, P., Romano, M., Ehrlich, I., Furgiuele, F., Gebbeken, N., Mechanical characterization of basalt fibre reinforced plastic with different fabric reinforcements, Tensile tests and FE-calculations with representative volume elements (RVEs), in: F. Iacovello, G. Risitano, L. Susmel (Eds.), *Acta Fracturae - XXII Convegno Nazionale IGF (Italiano Gruppo Frattura)*, Roma, (2013) 231-244.



- <http://www.gruppofrattura.it/ocs/index.php/cigf/IGF22/paper/view/10914/10241>.
- [22] Valentino, P., Sgambitterra, E., Furgiuele, F., Romano, M., Ehrlich, I., Gebbeken, N., Mechanical characterization of basalt woven fabric composites: numerical and experimental investigation, *Frattura ed Integrità Strutturale (Fracture and Structural Integrity)*, 8(28) (2014) 1-11. DOI:10.3221/IGF-ESIS.28.01.
- [23] Ottawa, P., Romano, M., Wagner, M., Ehrlich, I., Gebbeken, N., The influence of ondulation in fabric reinforced composites on dynamic properties in a mesoscopic scale in composites reinforced with fabrics on the damping behavior, in: DYNAMORE GmbH (Ed.), *Proceedings of the 11. LS- DYNA Forum*, Ulm, (2012) 171-172. <http://www.dynamore.de/de/download/papers/ls-dyna-forum-2012>
- [24] Romano, M., Micklitz, M., Olbrich, F., Bierl, R., Ehrlich, I., Gebbeken, N., Experimental investigation of damping properties of unidirectionally and fabric reinforced plastics by the free decay method, *Journal of Achievements in Materials and Manufacturing Engineering (JAMME)*, 63/2 (2014) 65-80. http://www.journalamme.org/vol63_2/6323.pdf
- [25] Romano, M., Micklitz, M., Olbrich, F., Bierl, R., Ehrlich, I., Gebbeken, N., Experimental investigation of damping properties of unidirectionally and fabric reinforced plastics by the free decay method, in: Meran, C. (ed.): *Proceedings of the 15th International Materials Symposium (IMSP'2014)*. Pamukkale University, Denizli, (2014) 665-679. http://imsp.pau.edu.tr/IMSP2014_Proceedings_Final_security.pdf
- [26] Romano, M., Charakterisierung von gewebeverstärkten Einzellagen aus kohlenstofffaserverstärktem Kunststoff (CFK) mit Hilfe einer mesomechanischen Kinematik sowie strukturdynamischen Versuchen, University of the Bundeswehr Munich, Department of Civil Engineering and Environmental Sciences, Neubiberg, (2016). <http://athene-forschung.unibw.de/doc/112760/112760.pdf>
- [27] Bronstein, I. N., Semendajew, K. A., *Taschenbuch der Mathematik*, seventh edition, Verlag Harri Deutsch, Frankfurt am Main, (2008).
- [28] Papula, L., *Mathematische Formelsammlung für Ingenieure und Naturwissenschaftler*, ninth edition, Vieweg+Teubner, Wiesbaden, (2006).
- [29] Büsching, F., Combined Dispersion and Reflection Effects at Sloping Structures, *Proceedings of ICPMRDT-International Conference on Port and Marine R&D and Technology*, Singapore, I (2001) 410-418.
- [30] Jones, R. M., *Mechanics of composite materials*, second edition, Taylor & Francis, Philadelphia, (1999).
- [31] Moser, K., *Faser-Kunststoff-Verbund, Entwurfs- und Berechnungsgrundlagen*, VDI-Verlag, Düsseldorf, (1992).
- [32] Schürmann, H., *Konstruieren mit Faser-Kunststoff-Verbunden*, Springer-Verlag, Berlin/Heidelberg/New York, (2005).
- [33] Stellbrink, K., *Micromechanics of Composites*, Hanser-Verlag, München/Wien, (1996).
- [34] N. N., *ANSYS 14.0 Help, Helpsystem of ANSYS Workbench Version 14.0.1*, SAS IP Inc., Canonsburg, (2011).
- [35] Barbero, E. J., *Introduction to Composite Materials Design*, second edition, CRC Press - Taylor & Francis Group, Boca Raton/London/New York, (2011).
- [36] Barbero, E. J., Luciano, R., Micromechanics Formulas for the Relaxation Tensor of linear Viscoelastic Composites with Transversely Isotropic Fibers, *International Journal of Solid Structures*, 32 (1995) 1859-1872.
- [37] Chamis, C. C., Simplified Composite Micromechanics Equations for Hygral, Thermal and Mechanical Properties, *NASA Technical Memorandum 83320* (1983) 1-10.
- [38] Chamis, C. C., Simplified Composite Micromechanics Equations for Hygral, Thermal and Mechanical Properties, *SAMPE Quarterly*, (1984) 14-23.
- [39] Tsai, S. W., Hahn, H. T., *Introduction to Composite Materials*, Technomic, (1980).
- [40] Foye, R. L., The transverse Poisson's ratio of composites, *Journal of Composites Materials*, 6 (1972) 293-295.

SYMBOLS AND NOMENCLATURE

The symbols and the nomenclature are indicated in alphanumerical order:

- 1, 2, 3 local principal directions
0, 1 states before and after deformation
a analytical
 A amplitude, area
 c composite
CFRP carbon fiber reinforced plastic
 D domain of definition



E	stiffness, Young's modulus
$E(\varphi, k)$	elliptic integral of the second kind
ε_x	longitudinal deformation as strain
$\varepsilon_{x,kin}$	difference of the applied and evaluated deformations in longitudinal direction
$\varepsilon_{y,kin}$	kinematic part due to mesomechanic geometric constraints in transversal direction
F	fabric, fill-yarn
f	fiber
FE	numerically determined by finite-element-analysis
φ_f	fiber volume content
G	shear modulus
H	absolute height
k_{el}	elastic support
kin	kinematic
l	length
L	longitudinal
λ	factor characterizing the type of the fabric
M, m	matrix
\tilde{M}	slope, sensitivity to the mesomechanic kinematic
max	maximum value
mod	modified value
n	substep
ν	Poisson's ratio
o	one-sided
\tilde{O}	degree of ondulation
PL	plain weave
PRS	plain representative sequence
rel	relative
R	roving
ρ	density
s	length of a function
S	wave steepness
T	transversal
tot	total
t	two-sided
u	displacement in longitudinal direction, degree of deformation
v	displacement in transverse direction in numerical investigations
w	displacement in transverse direction in analytical model, shift of the amplitude
W	warp-yarn
x, y, z	global principal directions